Ionics (2017) 23:1017–1025
DOI 10.1007/s11581-016-1885-9

ORIGINAL PAPER

Electrochemical deposition of carbon materials incorporated nickel sulfide composite as counter electrode for dye-sensitized solar cells

J. Theerthagiri[1] · R. A. Senthil[1] · Prabhakarn Arunachalam[2] · K. Amarsingh Bhabu[3] · A. Selvi[4] · J. Madhavan[1] · K. Murugan[5,6] · A. K. Arof[7]

Received: 25 August 2016 / Revised: 8 October 2016 / Accepted: 27 October 2016 / Published online: 6 December 2016
© Springer-Verlag Berlin Heidelberg 2016

Abstract The various carbon-based materials incorporated nickel sulfide (NiS) composites have been electrochemically deposited on fluorine-doped tin oxide (FTO) glass substrate. The structure, surface morphology, and elemental composition of the electrodeposited NiS composite materials were characterized by XRD, HR-SEM, and EDS. The electrochemically deposited various NiS composites such as NiS/AB (acetylene black), NiS/VC (Vulcan carbon), and NiS/MWCNT (multi walled carbon nanotubes) have been served as an efficient, low-cost counter electrode (CE) materials for dye-sensitized solar cells (DSSCs). Electrochemical impedance spectroscopy and cyclic voltammetry of NiS/AB CE composite materials exhibits a good conductivity and superior electrocatalytic performance over other various carbon incorporated materials. The positive synergistic effects, which increase the active catalytic sites and improved interfacial charge transfer, may be accountable for the superior electrocatalytic performance of NiS/AB composite materials The fabricated DSSC with NiS/AB CE reached a power conversion efficiency of 6.75%, which is equivalent with platinum electrode (7.20%). These results validate that the electrochemically deposited NiS/AB composite film is an auspicious alternative for low-cost and high efficient DSSCs.

Keywords Nickel sulfide · Acetylene black · Electrochemistry · Conversion efficiency · Polymer electrolyte · Dye-sensitized solar cell

✉ J. Madhavan
jagan.madhavan@gmail.com

[1] Solar Energy Lab, Department of Chemistry, Thiruvalluvar University, Vellore 632115, India

[2] Electrochemistry Research Group, Chemistry Department, College of Science, King Saud University, Riyadh 11451, Saudi Arabia

[3] Department of Physics, Manonmaniam Sundaranar University, Tirunelveli, Tamilnadu 627012, India

[4] Department of Biotechnology, DKM College for women, Vellore 632001, India

[5] Department of Zoology, Bharathiar University, Coimbatore, Tamilnadu 641046, India

[6] Present address: Thiruvalluvar University, Vellore 632115, India

[7] Department of Physics, Centre for Ionics University of Malaya, University of Malaya, 50603 Kuala Lumpur, Malaysia

Introduction

Nowadays, increasing global demands for energy and global warming concern have urged researchers to focus on clean and renewable energy resources. Solar energy is one of the most abundant energy resources, which can solve energy and environmental related issues [1, 2]. Dye-sensitized solar cell (DSSC) is one of the most favorable renewable energy devices and has received increasing attention among researchers due to its simple fabrication process, low cost, transparency, light weight, better plasticity, environmental friendliness, and capability in large-scale conversion of solar energy to electrical energy [3–5]. Commonly, a DSSC comprises of dye-sensitized TiO_2 photoelectrode, I^-/I_3^- redox electrolyte, and platinum (Pt) counter electrode. Under illumination condition, the photoexcited dye molecule introduces an electron into a conduction band (CB) of photoelectrode and the resultant dye molecule is reduced back by iodine/iodide electrolyte and the cycle is accomplished by the incessant flow of electrons from the photoelectrode to the counter electrode (CE) via external circuit [6–8]. The extensive research has been focused on all component of DSSC to advance the power conversion efficiency (PCE) and to lower the production cost. The CE is an indispensable component in DSSCs and

its role is to gather electrons from the external circuit and catalyze the reduction of I_3^- ion [9]. The CE with superior electrocatalytic performance over the reduction of I_3^- to I^- ions has decreased the device internal series resistance, which resulting in a high fill factor (FF) [10].

Generally, a Pt-deposited fluorine/indium-doped tin oxide (FTO/ITO) glass substrate is most commonly used as the CE in DSSCs [11]. Conversely, noble metal Pt can be easily corroded by I^-/I_3^- contained electrolytes and the high cost of Pt consumes 40% of the whole device fabrication cost [12, 13]. Moreover, the usage of Pt CE hinders the large-scale production and economical application of DSSCs. This promoted numerous studies to develop an alternative material to Pt CEs to reduce the cost and simultaneously keep the effectiveness of the DSSCs. Pt-free CE material includes carbon-based materials [14, 15], conducting polymers [16, 17], metal oxides [18], sulfides [5, 19, 20], selenides [21, 22], metal carbides [23], and nitrides [24]. Among the inorganic materials, nickel sulfides have been emerged as one of interesting metal sulfides due to its abundance in content, good conductivity, simple fabrication, and high electrocatalytic activity [19]. Many researchers have been studied on NiS-based Pt-free CEs for DSSCs in recent years [25–27]. The varieties of nickel sulfide phases have been formed depending on the synthetic conditions, such as NiS, NiS_2, Ni_3S_2, Ni_3N_4, and Ni_9S_8 [28, 29]. Hydrothermal and electrochemical depositions are the most widely used methods to synthesis of nickel sulfides. Very recently, Maiaugree et al. [30] reported that the carbon coated Ni_3S_2 as Pt-free CE for DSSCs and the film is fabricated via chemical bath deposition and an arc evaporation process. The fabricated DSSC with carbon/Ni_3S_2 CE attained a high PCE of 9.64%, which is higher than the Pt CE (8.38%). The enhancement of the PCE using carbon/Ni_3S_2 was mainly due to the fast electron transfer, high co-electrocatalytic activity, and large surface area of the materials. The addition of carbon as co-catalyst with Ni_3S_2 is the best way to assist the enhancement of I^-/I_3^- redox reaction. Xiao et al. [31] have deposited NiS/MWCNT on a titanium (Ti) foil substrate by a two-step process. Firstly, MWCNT was deposited on Ti substrate via electrophoresis method and followed by NiS deposition on MWCNTs surface via pulse potentiostatic method. The fabricated NiS/MWCNT/Ti hybrid film electrodes were served as a Pt-free CE in DSSCs. The DSSC with NiS/MWCNT/Ti CE attained a PCE of 7.90%, while the Pt/Ti CE attained 6.36%. Thus, the enhanced PCE of NiS/MWCNT/Ti hybrid film is mainly due to the synergistic effect of NiS/MWCNTs.

In the present investigation, we have electrochemically deposited NiS/AB, NiS/VC, and NiS/MWCNT composite film on FTO glass substrate by using cyclic voltammetry technique. Electrochemical deposition was preferred in this investigation because of its simple procedure, less cost, easy scale up and can control the electrochemically deposited structure by varying the operating conditions. The NiS/AB, NiS/VC, and NiS/MWCNT composite films were employed as Pt-free CE in DSSCs and examined the effect of the addition of various carbon-based materials as co-catalyst with NiS for an enhancement of PCE of DSSCs. Phthaloylchitosan (PhCh) was served as a polymer electrolyte solution for DSSCs. Though the higher PCE of the DSSCs has been achieved by employing liquid electrolytes (I^-/I_3^- redox couple) in DSSCs and its short-term stability, electrode corrosion and difficulty in sealing device limit the commercialization of DSSCs. The usage of polymer electrolyte can overcome these problems [7]. Herein, we report the comparison of electrodeposited NiS with various carbon materials as an efficient Pt-free CE for DSSCs.

Experimental section

Materials

Nickel(II) chloride hexahydrate ($NiCl_2.6H_2O$), thiourea (CH_2CSHCH_2), iodine (I_2), isopropanol, acetonitrile, and absolute ethanol were purchased from SDFCL, India. Acetylene black (Chevron, USA), MWCNT (Nanolab., Inc., USA), Vulcan XC-72 (Cabot, USA), chitosan (Merck, Germany), phthalic anhydride (Merck, Germany), and Carrbowax (Supelco, USA) were purchased from the respective company. N3 dye [cis-diisothiocyanato-bis(2,2′-bipyridyl-4,4′-dicarboxylic acid) ruthenium(II)], fluorine-doped SnO_2 (FTO) (7 Ω/square, TCO22-7) conducting glass, lithium iodide (LiI), and lithium perchlorate ($LiClO_4$) were acquired from Sigma Aldrich. Demineralized water was received from Nice chemicals, India.

Electrochemical deposition of NiS/carbon composite films

The electrochemical deposition of NiS/AB, NiS/VC, and NiS/MWCNT on FTO glass substrate was carried out in a single compartment cell with three-electrode assembly using a CHI608E electrochemical work station. The electrode setup comprises of a cleaned FTO-coated glass substrate as a working electrode (WE), a Pt-wire as a CE, and a saturated aqueous silver/silver chloride (Ag/AgCl) as a reference electrode (RE). The solution for electrochemical deposition was prepared by dispersing 5 mg of carbon material (AB/VC/MWCNT) in 50 mL of de-ionized water and sonicated for 30 min. Then, $NiCl_2.6H_2O$ (0.05 M) and thiourea (1.0 M) were added into the carbon-dispersed solution. The potential range of cyclic voltammetry electrochemical deposition of NiS/carbon composites was performed from −0.9 to 0.7 V at a scan rate of 0.05 Vs^{-1} for 25 cycles. The as-prepared NiS/AB, NiS/VC, and NiS/MWCNT electrodes were rinsed in demineralized water and dried at room temperature for 2 h. For comparison,

the bare NiS film was also electrochemically deposited under same condition.

Preparation of polymer electrolyte

The phthaloylchitosan (PhCh)-based polymer electrolyte was used as an electrolyte for the fabrication of DSSCs in this investigation. Polymer electrolyte composition was discussed in our earlier reports [32, 33].

Characterization techniques

The X-ray diffraction (XRD) patterns were logged via Rigaku X-ray diffractometer (Mini Flex II) with Cu Kα radiation (λ = 0.54 nm) in the 2θ range 10–80° at a scan rate of 5°/min. The shape and morphology of the sample were examined by using FEI Quanta FEG 200-high resolution scanning electron microscope (HR-SEM) at an accelerating voltage of 20 kV. The elemental compositions of electrochemically deposited samples were analyzed using an energy dispersive X-ray spectroscopy (EDS) equipped with HR-SEM. The electrocatalytic activity of the materials was assessed by cyclic voltammetry (CV) in electrochemical work station (CHI608E). The CV was carried out in a three-electrode assembly in acetonitrile solution containing 0.1 M $LiClO_4$, 10 mM LiI, and 1.0 mM I_2 in work station in the potential ranging from −1.3 to +1.2 V at a scan rate of 150 mVs^{-1}. The polymer electrolyte solution was purged with N_2 gas for 30 min prior to CV measurements.

Assembly of DSSCs

The TiO_2 photoelectrode was prepared on the FTO substrates in two layers. Firstly, the TiO_2 compact layer was arranged by the addition of TiO_2 (0.5 g, P90) powder with 2 mL of HNO_3 (0.1 M) and grinding well for 30 min. Then, the obtained paste was spin coated on FTO glass substrate at 2650 rpm for 60 s and then sintered at 450 °C for 30 min. The obtained TiO2 compact layer on FTO improves adhesion and also inhibits the back electron flow from FTO into electrolyte solution [3]. Secondly, the TiO_2 paste for the second porous layer was fabricated by grinding of 0.5 g of TiO_2 (P25) with 2 mL of 0.1 M HNO_3, 0.1 g carbowax, and 2 drops of Triton-X 100. Then, the obtained TiO_2 (P25) paste was coated above the compact layer via doctor blade technique and followed by sintering at 450 °C for 30 min. The prepared TiO_2 photoanode was dye sensitized by immersing in 3×10^{-4} M ethanol solution of N3 dye for 24 h, and then, the dye-sensitized TiO_2 electrodes were rinsed with absolute ethanol and dried in the air before assembling with different CEs. A sandwich-type configuration of DSSCs was gathered by clamping both the dye-sensitized TiO_2 photoanode and CE. Prior to the assembly, the polymer electrolyte was evenly spread on the surface of dye-sensitized TiO_2 photoanode. In addition, Pt CE was prepared by spin coating of plastisol solution on FTO plate and sintered at 500 °C for 30 min and this was used as a reference cell for comparison studies. The effective cell area was 0.2 cm^2 and photovoltaic measurements were completed in the open air atmosphere. The cell configuration of the fabricated DSSC is as follows:

FTO/TiO_2/N3/polymer electrolyte/NiS/FTO
FTO/TiO_2/N3/polymer electrolyte/NiS-AB/FTO
FTO/TiO_2/N3/polymer electrolyte/Pt/FTO

The photocurrent density-voltage (*J-V*) characteristics of the DSSCs were measured under an illumination of 1 sun (100 mW/cm^2) using a PEC-L01 (PECCELL Inc., Japan) solar simulator. The photovoltaic parameters (i.e., fill factor (FF) and overall PCE (η) of the fabricated DSSCs are calculated and it was described in our earlier reports [34, 35].

Results and discussion

XRD studies

The XRD patterns of pure FTO glass substrate, the electrochemically deposited NiS, NiS/AB, NiS/VC, and NiS/MWCNT, are shown in Fig. 1. The diffraction peaks of NiS and carbon NiS composite films can be observed at 2θ = 30.2°, 46.1°, and 53.6°, which can be indexed to the (100), (102), and (110) diffraction planes of NiS (JCPDS No. 75-0613). These diffraction peaks are in good agreement with earlier report by Xiao et al. [11]. All other strong diffraction peaks correspond to the pure FTO glass substrate. The XRD patterns of NiS in NiS/AB, NiS/VC, and NiS/MWCNT

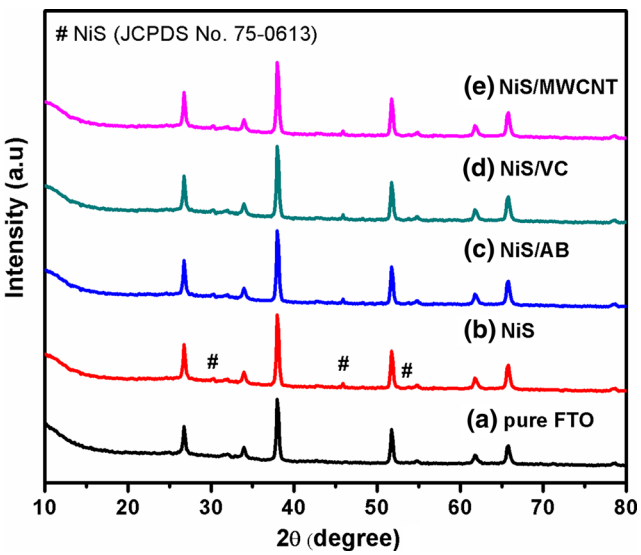

Fig. 1 XRD patterns of *(a)* pure FTO glass substrate, electrodeposited, *(b)* NiS, *(c)* NiS/AB, *(d)* NiS/VC, and *(e)* NiS/MWCNT films

(Fig. 1c–e) are unaltered with the incorporation of different carbon materials suggesting that the low content of carbon with dense covering of NiS on its surface and with no specific diffraction peaks of carbon in the NiS/C samples was observed. However, it can be noted that the little changes in the peak intensity of NiS/FTO were noticed which may be due to the incorporation of carbon atoms at the interstitial positions or substitutional sites producing considerable contraction and expansion of the lattice constants.

Morphology and elemental studies

The shape and surface morphology of the electrochemically deposited NiS and NiS/AB were observed by HR-SEM. The characteristic HR-SEM images of NiS and NiS/AB films are presented in Fig. 2a, b. The SEM images appear to be tight and random distribution of NiS over the surface of FTO glass substrate. The pure NiS (Fig. 2a) exhibited a spherical shape with some aggregated particles comprising of a large number of irregular smaller particles having a size of ~200 nm. The morphology of NiS/AB (Fig. 2b) clearly shows that the addition of AB into NiS does not change its morphology. It can be seen that NiS/AB appeared in spherical shape and the average particle size of the electrodeposited NiS/AB varied between 50 and 200 nm. It can be evidenced from the SEM analysis that NiS/AB shows smaller particle size with less agglomeration of particles on incorporating carbon content into pure NiS. The surface morphology of the electrochemically deposited NiS and NiS/AB layer was observed as good adhesion on the FTO glass substrate. Adhesion plays a significant role in the electrochemical deposition of thin films. The good adhesion of the electrocatalytic material on FTO glass substrate is a key factor for defining the long-term stability and efficiency of the DSSCs, when these films are used as CEs.

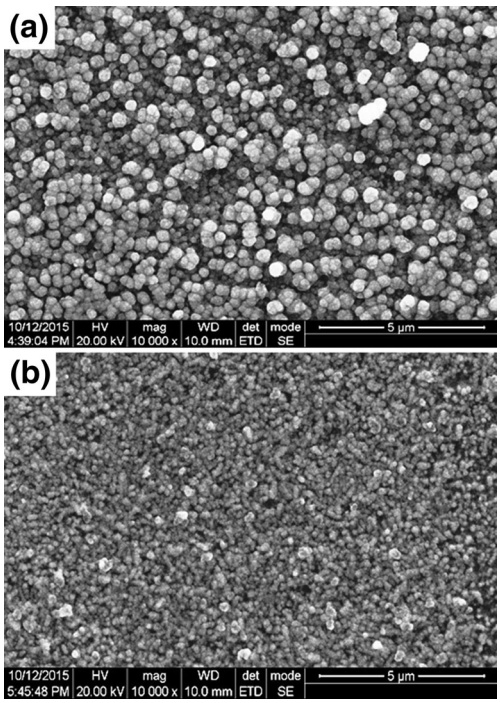

Fig. 2 Typical HR-SEM images of electrochemically deposited **a** NiS and **b** NiS/AB films

The elemental analysis of electrochemically deposited NiS and NiS/AB was examined by EDS and the obtained results are presented in Fig. 3a, b. The formation of NiS on the surface of FTO glass substrate was confirmed from EDS results (Fig. 3a). It clearly showed that NiS consisted of Ni and S atoms and NiS/AB composed of Ni, S, and C atoms only (Fig. 3b). In addition, the observed other peaks of Sn, O, Si, and F are ascribed to the FTO substrate [2], and no other impurity peaks are found. The atomic ratios of species noticed by EDS are displayed in Fig. 3 inset. We can conclude from the XRD and EDS results that NiS and NiS/AB are well deposited on the surface of FTO glass substrate.

Cyclic voltammetry studies

The electrocatalytic activity of the synthesized CE materials towards the reduction of I_3^- to I^- ions was assessed using CV studies. The cyclic voltammograms of the bare NiS, NiS-AB, NiS/VC, NiS/MWCNT, and Pt electrodes for I^-/I_3^- redox couple are shown in Fig. 4. Typically, there are two pairs of oxidation and reduction peaks (Ox-1/Red-1, Ox-2/Red-2, as labeled in Fig. 4) that were witnessed for all the electrodes. It can be seen that the obtained redox peaks of NiS, NiS/AB, NiS/VC, and NiS/MWCNT are similar to Pt, suggesting a similar electrocatalytic behavior for the I_3^- reduction. The pair of redox peaks observed at left side at low potential (Ox-1/Red-1) could be attributed to the redox reaction shown in Eq. (1), and the pair of redox peaks observed at right side at high potential (Ox-2/Red-2) are ascribed to the redox reaction shown in Eq. (2), respectively.

$$I_3^- + 2e^- \leftrightarrow 3I^- \tag{1}$$

$$3I_2 + 2e^- \leftrightarrow 2I_3^- \tag{2}$$

The characteristic peaks of Ox-1 and Red-1 are at great observation in our measurements because the CE is accountable for the catalyzing reduction of I_3^- to I^- ions in DSSCs [5]. The peak current density and peak-to-peak separation (E_{pp}) are two significant parameters to assess the electrocatalytic performance of various CEs [19].

The higher peak current density and lower E_{pp} values are beneficial for the CE to achieve high catalytic performance. The observed E_{pp} values for NiS, NiS/AB, NiS/VC, NiS/MWCNT, and Pt CEs were recorded in Table 1. It can be seen that NiS/AB CE exhibited higher peak current density and smaller E_{pp} (0.78 V) than the NiS, NiS/VC, and NiS/MWCNT and almost similar to Pt CE indicating that NiS/

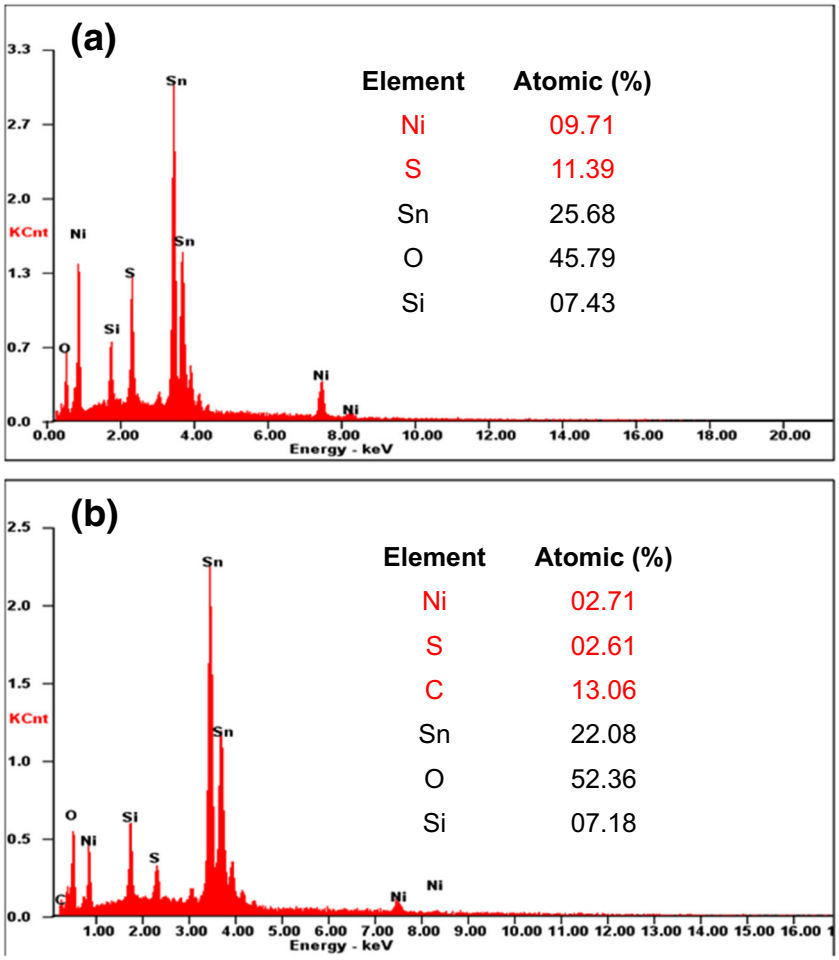

Fig. 3 EDS spectra of electrochemically deposited **a** NiS and **b** NiS/AB films

AB CE can show better electrocatalytic activity for I_3^- reduction than other CEs. This may be due to a positive synergetic effect offered when NiS and AB are combined together, and this increases the active catalytic sites and improves interfacial charge-transfer rate. Zuo et al. [19] synthesized NiS/RGO via solvothermal route and Li et al. [5] for NiS_2/RGO composite synthesized via hydrothermal route.

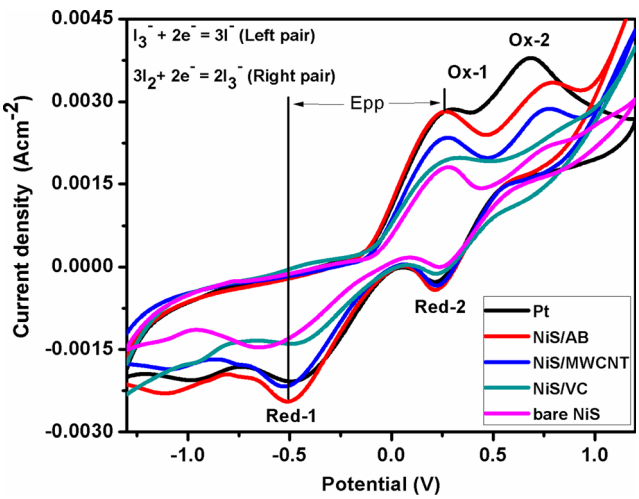

Fig. 4 Cyclic voltammograms for bare NiS, NiS/VC, NiS/MWCNT, NiS/AB, and Pt CEs at a scan rate of 150 mVs^{-1} in 10 mM LiI, 1 mM I_2, and 0.1 M $LiClO_4$ as supporting electrolyte in acetonitrile

Figure 5a shows the cyclic voltammograms of NiS/AB CE for I^-/I_3^- redox system at various scan rates. It can be seen that the cathodic and anodic peaks gradually and regularly shifted to the negative and positive direction with increasing scan rates indicating the inner sites of the sulfide electrodes becomes more reactive in a high scan rate [25]. Figure 5b displays the linear relationship between the peak current density versus square root of the scan rates and it reveals the diffusion limitation of the redox reactions, which affect the transport of I^- on the CE surface [36].

Table 1 Electrochemical parameters for different CEs

CEs	E_{pp} (V)	R_s (Ω)	R_{ct} (Ω)	R_b (Ω)
NiS	0.92	8.50	86.29	94.8
NiS/AB	0.78	7.67	63.42	71.1
NiS/VC	0.82	7.17	72.42	79.6
NiS/MWCNT	0.80	6.59	71.40	78.0
Pt	0.77	8.71	61.58	70.3

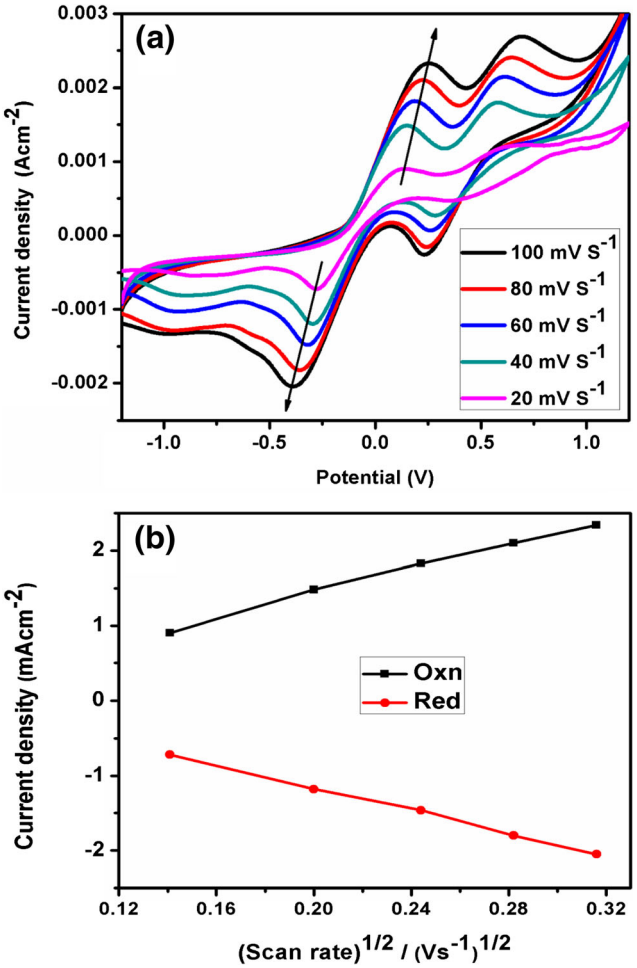

Fig. 5 **a** Cyclic voltammograms for NiS/AB electrode at different scan rates. **b** Relationship between redox peak current vs. square root of the scan rates

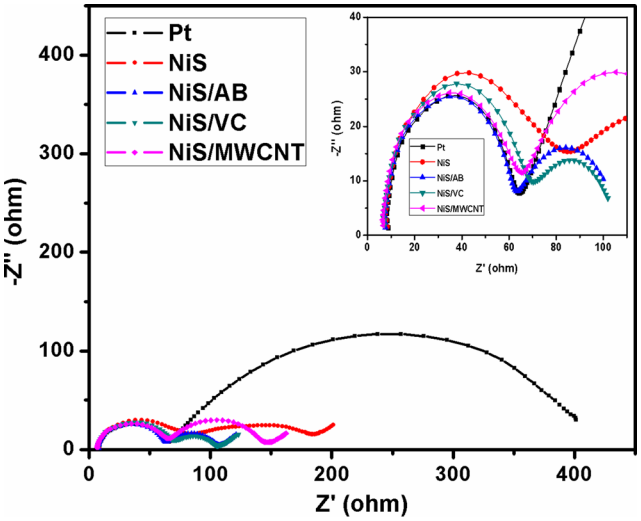

Fig. 6 Nyquist plots of EIS for bare NiS, NiS/AB, NiS/VC, NiS/MWCNT, and Pt CEs. *Inset* shows the zoomed view of lower part of the Nyquist spectra

Electrochemical impedance spectroscopy studies

The electrochemical impedance spectroscopy (EIS) measurements were further performed to evaluate the electrocatalytic activity of the electrochemically deposited NiS, NiS/AB, NiS/VC, NiS/MWCNT, and Pt CEs. The EIS is a powerful technique to investigate internal resistance, charge-transfer process, and correlation between the electrocatalytic activities of the CEs [37]. Figure 6 shows the Nyquist plot of EIS for different CEs. The enlarged view of lower part of the spectra is displayed in the inset of Fig. 6. Generally, the high-frequency intercept on the real axis (Z′-axis) agrees to the series resistance (R_s), and the high-frequency region of semicircle (left side) is attributed to the charge-transfer resistance (R_{ct}) at the CE/electrolyte interface [5, 36]. The R_s and R_{ct} are mainly composed of the bulk resistance (R_b) of the CE materials. The Nyquist plots were fitted by the Z-view software to obtain the EIS parameters and the corresponding resistances (R_s and R_{ct}) are listed in Table 1. It can be noted that all CEs have closely same R_s value, and therefore, the effect on photovoltaic performance by the R_s can be omitted [38]. However, the R_{ct} values are different for different electrodes. The R_{ct} value is actually related to the electrocatalytic activity for the reduction of I_3^- to I^- ions. A lower R_{ct} value means higher electrocatalytic activity and higher charge-transfer rate between the CE and electrolyte [25].

In Nyquist plot, the high-frequency region of the first semicircle represents the electron transfer from the counter electrode to I_3^- ions in the electrolyte, that is, the charge-transfer resistances at the CE/electrolyte interface. The second (large) semicircle represents the charge recombination between the injected electrons in TiO_2 and I_3^- ions in the electrolyte, that is, the charge-transfer resistances at the TiO_2/dye/electrolyte interface. In our study, the characteristics of the first semicircle are the focus of our analysis because the CE material with low R_{ct} value at the CE/electrolyte interface provides high electrocatalytic activity for the reduction of I_3^- to I^- ions in DSSCs. In the present study, the electrodeposited NiS/AB electrode showed the lowest R_{ct} value (63.42 Ω) than pure NiS, NiS/VC, and NiS/MWCNT electrodes and close to Pt CE (61.58 Ω). Hence, the NiS/AB would be expected to show higher electrocatalytic activity for I_3^- reduction than NiS and other carbon incorporated NiS materials. The observed EIS results are in well accordance with the results obtained from CV measurements.

DSSC studies

The graphic representation of the electron transfer mechanism of DSSCs with NiS/AB CE is presented in Fig. 7. Under illumination condition, the photoexcited N3 dye molecule introduces an electron into a CB of TiO_2 photoelectrode and the resultant dye molecule is reduced back by iodine/iodide electrolyte and the cycle is accomplished by the incessant flow of electrons from the TiO_2 photoelectrode to the NiS/AB CE via external circuit.

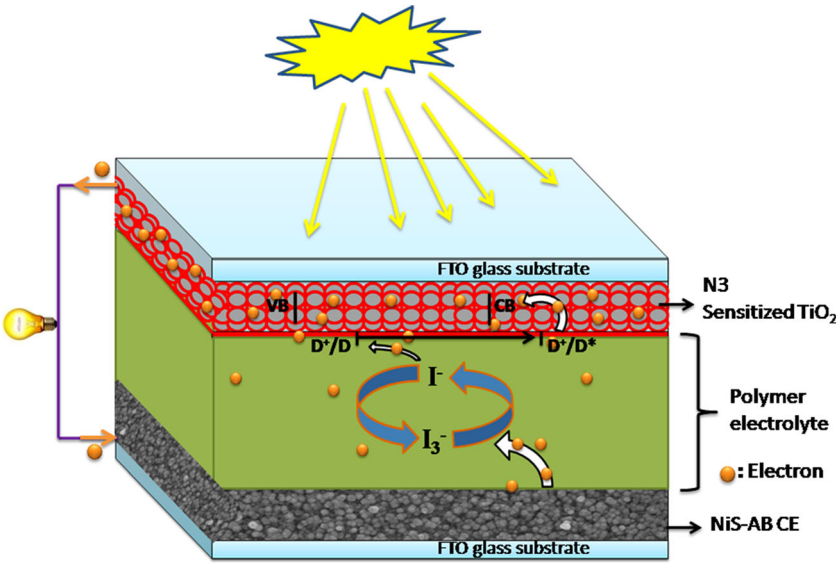

Fig. 7 The schematic illustration of the electron transfer mechanism taking place in the fabricated DSSCs

The photovoltaic performances of fabricated DSSCs were analyzed by assessing the photocurrent density-voltage (*J-V*) curves. The *J-V* curves obtained for the DSSCs with NiS, NiS/AB, and Pt CEs are presented in Fig. 8, and the corresponding photovoltaic parameters such as V_{oc}, J_{sc}, FF, and η are summarized in Table 2. The photovoltaic parameters of fabricated DSSC with NiS/AB CE exhibited power conversion efficiency (PCE) of 6.75% with V_{oc} of 0.72 V, J_{sc} of 14.01 mA/cm^2, and FF of 0.67. The observed photovoltaic performance using NiS/AB CE was comparable to the Pt CE, which gives a PCE of 7.20% with V_{oc} of 0.66 V, J_{sc} of 17.32 mA/cm^2, and FF of 0.63. The improved PCE of NiS/AB CE is mainly due to an improved FF and V_{oc}, which could arise from the more active catalytic sites and improved interfacial charge transfer by the combination of NiS and AB. This result suggests that the electrodeposited NiS/AB on FTO is a favorable substitute electrocatalyst to the Pt-free CE in DSSCs.

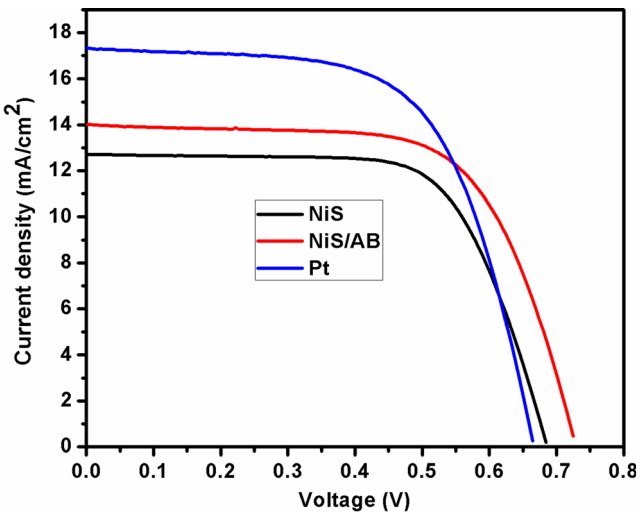

Fig. 8 Photocurrent-voltage curve of DSSCs fabricated with NiS, NiS/AB, and Pt CEs

Conclusions

In summary, the various carbon materials (AB, VC, MWCNT) incorporated NiS composites were fabricated on FTO glass substrate by a simple electrochemical deposition using cyclic voltammetry studies. The electrochemically deposited sulfide materials were characterized by XRD, HR-SEM, and EDS studies. Subsequently, the electrochemically deposited NiS, NiS/AB, NiS/VC, and NiS/MWCNT films were applied as a Pt-free low-cost CE for DSSCs. The CV and EIS measurements revealed that the NiS/AB CE exhibited an excellent electrocatalytic activity and have good conductivity for the reduction of I_3^- to I^- ions than the bare NiS, NiS/VC, and NiS/MWCNT. The NiS/AB composite offered positive synergistic effects, which increases the active catalytic sites and improves the interfacial charge-transfer rate. The PCE of DSSC fabricated with NiS/AB CE achieved a 6.75%, which is equivalent with Pt CE (7.20%). The observed results indicated that electrochemically deposited NiS/AB composite film can be a favorable substitute to Pt electrode for low-cost and high efficient DSSCs.

Table 2 The photovoltaic parameters of DSSCs fabricated with different CEs

Counter electrode	V_{oc} (*V*)	J_{sc} (mA/cm^2)	Fill factor	Efficiency, η (%)
NiS	0.68 ± 0.02	12.71 ± 0.04	0.69 ± 0.03	5.96 ± 0.01
NiS/AB	0.72 ± 0.02	14.01 ± 0.02	0.67 ± 0.02	6.75 ± 0.01
Pt	0.66 ± 0.02	17.32 ± 0.03	0.63 ± 0.03	7.20 ± 0.01

Acknowledgements We gratefully acknowledge the financial support from the Department of Atomic Energy-Board of Research in Nuclear Sciences (DAE-BRNS) (Grant No. 2013/37P/1/BRNS/10), Mumbai, India. Also, this study was supported by the Deanship of Scientific Research, College of Science Research Centre, King Saud University, Saudi Arabia.

References

1. Joshi P, Xie Y, Ropp M, Galipeau D, Bailey S, Qiao Q (2009) Dye-sensitized solar cells based on low cost nanoscale carbon/TiO_2 composite counter electrode. Energy Environ Sci 2:426–429
2. Jiang N, Bogoev L, Popova M, Gul S, Yano J, Sun Y (2014) Electrodeposited nickel-sulfide films as competent hydrogen evolution catalysts in neutral water. J Mater Chem A 2:19407–19414
3. Theerthagiri J, Senthil RA, Buraidah MH, Madhavan J, Arof AK (2015) Effect of tetrabutylammonium iodide content on PVDF-PMMA polymer blend electrolytes for dye-sensitized solar cells. Ionics 21:2889–2896
4. Anuratha KS, Mohan S, Panda SK (2016) Pulse reverse electrodeposited $NiCo_2S_4$ nanostructures as efficient counter electrodes for dye-sensitized solar cells. New J Chem 40:1785–1791
5. Li Z, Gong F, Zhou G, Wang ZS (2013) NiS_2/reduced graphene oxide nanocomposites for efficient dye-sensitized solar cells. J Phys Chem C 117:6561–6566
6. Lee WJ, Ramasamy E, Lee DY, Song JS (2008) Performance variation of carbon counter electrode based dye-sensitized solar cell. Sol Energy Mater Sol Cells 92:814–818
7. Theerthagiri J, Senthil AR, Madhavan J, Maiyalagan T (2015) Recent progress in non-platinum counter electrode materials for dye-sensitized solar cells. ChemElectroChem 2:928–945
8. Gong F, Xu X, Li Z, Zhou G, Wang ZS (2013) $NiSe_2$ as an efficient electrocatalyst for a Pt-free counter electrode of dye-sensitized solar cells. Chem Commun 49:1437–1439
9. He J, Duffy NW, Pringle JM, Cheng YB (2013) Conducting polymer and titanium carbide-based nanocomposites as efficient counter electrodes for dye-sensitized solar cells. Electrochim Acta 105: 275–281
10. Jeong I, Lee J, Joseph KLV, Lee HI, Kim JK, Yoon S, Lee J (2014) Low-cost electrospun WC/C composite nanofiber as a powerful platinum-free counter electrode for dye sensitized solar cell. Nano Energy 9:392–400
11. Xiao Y, Wang C, Han G (2015) Effects of thiourea concentration on electrocatalytic performances of nickel sulfide counter electrodes for use in dye-sensitized solar cells. Mater Res Bull 61:326–332
12. Lin JY, Liao JH, Chou SW (2011) Cathodic electrodeposition of highly porous cobalt sulfide counter electrodes for dye-sensitized solar cells. Electrochim Acta 56:8818–8826
13. Murakami TN, Ito S, Wang Q, Nazeeruddin MK, Bessho T, Cesar I, Liska P, Humphry-Baker R, Comte P, Pechy P, Grätzel M (2006) Highly efficient dye-sensitized solar cells based on carbon black counter electrodes. J Electrochem Soc 153:A2255–A2261
14. Wang G, Zhang J, Kuang S, Zhuo S (2015) Nitrogen-doped porous carbon prepared by a facile soft-templating process as low-cost counter electrode for high-performance dye-sensitized solar cells. Mater Sci Semicond Process 38:234–239
15. Gao Y, Raissan M, Hamed W, Yang Z, Cheng Z, Sen Ruan S (2015) Layer-by-layer deposition of CNT^- and CNT^+ hybrid films for platinum free counters electrodes of dye-sensitized-solar-cells. RSC Adv 5:95551–95557
16. Saranya K, Md R, Subramania A (2015) Developments in conducting polymer based counter electrodes for dye-sensitized solar cells—an overview. Eur Polym J 66:207–227
17. Lan Z, Gao S, Wu J, Lin J (2015) High-performing dye-sensitized solar cells based on reduced graphene oxide/PEDOT-PSS counter electrodes with sulfuric acid post-treatment. J Appl Polym Sci 132:42648
18. Shahpari M, Behjat A, Khajaminian M, Torabi N (2015) The influence of morphology of hematite (α-Fe_2O_3) counter electrodes on the efficiency of dye-sensitized solar cells. Sol Energy 119:45–53
19. Zuo X, Zhang R, Yang B, Li G, Tang H, Zhang H, Wu M, Ma Y, Jin S, Zhu K (2015) NiS nanoparticles anchored on reduced graphene oxide to enhance the performance of dye-sensitized solar cells. J Mater Sci Mater Electron 26:8176–8181
20. Banerjee A, Upadhyay KK, Bhatnagar S, Tathavadekar M, Bansode U, Agarkar S, Ogale SB (2014) Nickel cobalt sulphide nanoneedle array as an effective alternative to Pt as a counter electrode in dye-sensitized solar cells. RSC Adv 4:8289–8294
21. Theerthagiri J, Senthil RA, Susmitha K, Raghavender M, Madhavan J (2015) Synthesis of efficient $Ni_{0.9}X_{0.1}Se_2$ (X = Cd, Co, Sn and Zn) based ternary selenides for dye-sensitized solar cells. Mater Sci Forum 832:61–71
22. Dong J, Wu J, Jia J, Wu S, Zhou P, Tu Y, Lan Z (2015) Cobalt selenides nanorods used as a high efficient counter electrode for dye-sensitized solar cells. Electrochim Acta 168:69–75
23. Liao Y, Pan K, Wang L, Pan Q, Zhou W, Miao X, Jiang B, Tian C, Tian G, Wang G, Fu H (2013) Facile synthesis of high-crystallinity graphitic carbon/Fe_3C nanocomposites as counter electrodes for high-efficiency dye-sesnitized solar cells. ACS Appl. Mater Interfaces 5:3663–3670
24. Li GR, Song J, Pan GL, Gao XP (2011) Highly Pt-like electrocatalytic activity of transition metal nitrides for dye-sensitized solar cells. Energy Environ Sci 4:1680–1683
25. Hu Z, Xia K, Zhang J, Hu Z, Zhu Y (2015) Highly transparent ultrathin metal sulfide films as efficient counter electrodes for bifacial dye-sensitized solar cells. Electrochim Acta 170:39–47
26. Lu MN, Dai CS, Tai SY, Lin TW, Lin JY (2014) Hierarchical nickel sulfide/carbon nanotube nanocomposite as a catalytic material toward triiodine reduction in dye-sensitized solar cells. J Power Sources 270:499–505
27. Haritha MV, Chandu Gopi VVM, Kim SK, Lee JC, Kim HJ (2015) Solution-processed morphology-controllable nanosphere structured highly efficient and stable nickel sulfide counter electrodes for dye- and quantum dot-sensitized solar cells. New J Chem 39:9575–9585
28. Huo J, Wu J, Zheng M, Tu Y, Lan Z (2015) Effect of ammonia on electrodeposition of cobalt sulfide and nickel sulfide counter electrodes for dye-sensitized solar cells. Electrochim Acta 180:574–580
29. Sun H, Qin D, Huang S, Guo X, Li D, Luo Y, Meng Q (2011) Dye-sensitized solar cells with NiS counter electrodes electrodeposited by a potential reversal technique. Energy Environ Sci 4:2630–2637
30. Maiaugree W, Tangtrakarn A, Lowpa S, Ratchapolthavisin N, Amornkitbamrung V (2015) Facile synthesis of bilayer carbon/Ni_3S_2 nanowalls for a counter electrode of dye-sensitized solar cell. Electrochim Acta 174:955–962
31. Xiao Y, Wu J, Lin J, Yue G, Lin J, Huang M, Huang Y, Lan Z, Fan L (2013) A high performance Pt-free counter electrode of nickel sulfide/multi-wall carbon nanotube/titanium used in dye-sensitized solar cells. J Mater Chem A 1:13885–13889
32. Theerthagiri J, Senthil RA, Buraidah MH, Madhavan J, Arof AK, Ashokkumar M (2016) One-step electrochemical deposition of $Ni_{1-x}Mo_xS$ ternary sulfides as an efficient counter electrode for dye-sensitized solar cells. J Mater Chem A. doi:10.1039/C6TA04405K
33. Theerthagiri J, Senthil RA, Prabhakarn A, Madhavan J, Buraidah MH, Amutha S, Arof AK (2016) Synthesis of various carbon incorporated flower-like MoS_2 microspheres as counter electrode for dye-sensitized solar cells. J Solid State Electrochem. doi:10.1007/s10008-016-3407-0

34. Theerthagiri J, Senthil RA, Buraidah MH, Madhavan J, Arof AK (2015) Studies of solvent effect on the conductivity of 2-mercaptopyridine-doped solid polymer blend electrolytes and its application in dye-sensitized solar cells. J Appl Polym Sci 132:42489
35. Senthil RA, Theerthagiri J, Madhavan J (2016) Organic dopant added polyvinylidene fluoride based solid polymer electrolytes for dye-sensitized solar cells. J Phys Chem Solids 89:78–83
36. Wang W, Pan X, Liu W, Zhang B, Chen H, Fang X, Yao J, Dai S (2014) $FeSe_2$ films with controllable morphologies as efficient counter electrodes for dye-sensitized solar cells. Chem Commun 50:2618–2620
37. Yang X, Luo J, Zhou L, Yang B, Zuo X, Li G, Tang H, Zhang H, Wu M, Ma Y, Jin S, Sun Z, Chen X (2014) A novel Pt-free counter electrode for dye-sensitized solar cells: nickel sulphide hollow spheres. Mater Lett 136:241–244
38. Gong F, Wang H, Xu X, Zhou G, Wang ZS (2012) In situ growth of $Co_{0.85}Se$ and $Ni_{0.85}Se$ on conductive substrates as high-performance counter electrodes for dye-sensitized solar cells. J Am Chem Soc 134:10953–10958